GEOMETRIC VALIDATION OF IMAGERY AND PRODUCTS FROM A HIGH PERFORMANCE AIRBORNE DIGITAL SENSOR

J. P. Mills [a, *], S. Alhamlan [b], A. S. Abuoliat [b], J. Horgan [c]

[a] University of Newcastle upon Tyne, School of Civil Engineering and Geosciences, UK - j.p.mills@ncl.ac.uk
[b] General Survey Committee, Riyadh, Kingdom of Saudi Arabia - hamlans88@hotmail.com, abuoliat@gmail.com
[c] Ordnance Survey, Romsey Road, Southampton, UK - jon.horgan@ordnancesurvey.co.uk

Commission I, WG I/4

KEY WORDS: Aerial, Aerial Digital Cameras, DEM/DTM, LIDAR, Photogrammetry, Sensors, Three-Line, Triangulation

ABSTRACT:

This paper describes a geometric evaluation of the photogrammetric workflow resulting from an experimental aerial survey performed using a Leica Airborne Digital Sensor (ADS40) system. Imagery of a 13 km^2 study area in the United Kingdom was captured using an ADS40. The study area was flown with the ADS40 at four different altitudes with resulting imagery at ground sampled distances of 15, 20, 25 and 30 cm. Ground points, comprising natural features distributed throughout the study area, were surveyed using GPS methods. In addition, RC30 film imagery and data from a lidar survey conducted using an Optech ALTM 2050 airborne laser scanner was also available for use in validation. The ADS40 imagery of the study area was processed using standard commercial software and a number of tests were conducted to geometrically assess the photogrammetric performance of imagery from the sensor at various stages throughout the photogrammetric workflow. Experiments examined the influence of ground control points (GCPs) in bundle block adjustment and the performance of digital elevation models (DEMs) resulting from the processing of ADS40 imagery. This independent research has permitted a series of initial conclusions to be drawn and preliminary recommendations to be made for optimum deployment of the ADS40 sensor under certain operational conditions. For example, it is shown that, despite advances made in direct positioning and orientation using integrated satellite and inertial surveying, the importing of GCPs into the block adjustment process remains a critical issue influencing the achievable accuracy during photogrammetric measurement.

1. INTRODUCTION

This paper reports on research into the geometric evaluation of the photogrammetric workflow and products resulting from an experimental aerial survey performed using a Leica Airborne Digital Sensor (ADS40) system (Sandau et al., 2000). A number of tests were conducted to geometrically assess the photogrammetric performance of imagery from the sensor at various stages throughout the photogrammetric flow line. Initial experiments follow on from previously reported research that examined the influence of ground control points (GCPs) in bundle block adjustment (Alhamlan et al., 2004). Further testing examined the performance of photogrammetric products, namely digital elevation models (DEMs) and orthoimagery, resulting from the processing of ADS40 imagery. Only the results of DEM product evaluation are reported in this paper.

2. STUDY AREA

Imagery of the study area, a region of Bristol in the United Kingdom covering approximately 13 km^2 (Figure 1), was captured using an ADS40 in September 2003. The study area was flown with the ADS40 to provide resulting imagery at nominal ground sampled distances (GSDs) of 15, 20, 25 and 30 cm (i.e. four different altitudes of approximately 1500 m, 2000, 2400 m and 2900 m with the sensor's 62.5 mm focal length and 6.5 μm pixel size). At 15 cm GSD, the dataset consists of four adjacent strips of imagery; at 20 cm GSD, three adjacent strips; and at 25 and 30 cm, two adjacent strips.

Figure 1. Overview of study area.

A total of 49 ground points, natural features distributed throughout the study area, were surveyed by Ordnance Survey using GPS methods and coordinates provided for the study in the OSGB36 National Grid system. Unfortunately, a number of these points were either un-measurable from the ADS40 imagery recorded at smallest scale, or were not visible at some scales due to being missed from the periphery

* Corresponding author.

of the survey. As a result, only 30 points were used in subsequent analysis. For consistency, 12 of these were used as ground control points (GCPs), measured in different configurations, and 18 as independent check points (ICPs). It is the norm to use many more points than this in order to provide statistical relevant results (e.g. Cramer, 2005), so for further validation purposes, Ordnance Survey also provided OSGB36 DEM data from a lidar survey conducted using an Optech ALTM 2050 airborne laser scanner in November 2004 (sample shown in Figure 2).

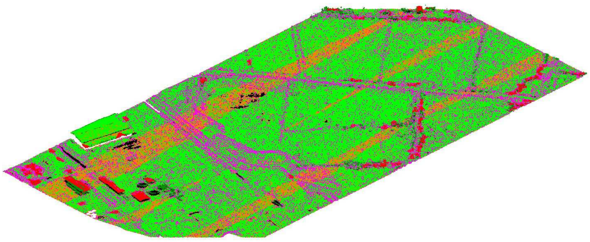

Figure 2. Sample of OPTECH data for the Bristol study area.

Moreover, 1: 3000 scale film imagery captured using a RC30 camera in April 2003, was provided. This was made available in analogue form for analytical photogrammetric processing and also in digital form (scanned at 21 µm giving a GSD of approximately 6 cm) for digital processing. However this imagery was not used to derive the results presented here

3. METHODOLOGY

3.1 Accuracy of direct orientation

The raw ADS40 images were first resampled to remove the influences of the aircraft movement during image acquisition. This was performed using position and attitude data from a variant of the Applanix Position and Orientation System (POS) developed to meet the requirements of the ADS40 sensor (Sandau et al., 2000). Data was collected synchronously with image acquisition and processed relative to a GPS base station. Rectification of the ADS40 imagery was performed, in order to produce stereo-viewable images, using GPro.

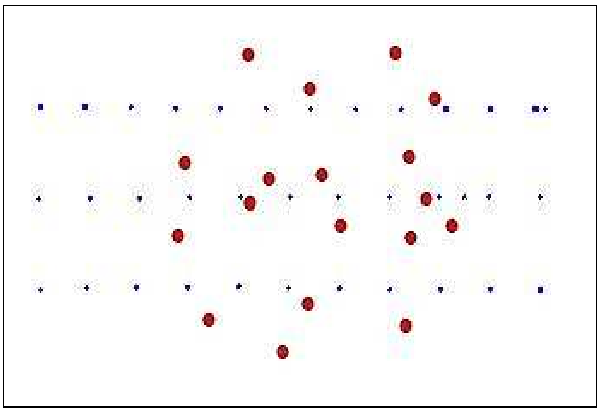

Figure 3. Location of ICPs (red dots) in relation to flight lines represented by IPOS position fixes (blue dots).

Using the forward and backward looking panchromatic images (resulting in a 42º stereo angle.) from the 20 cm GSD ADS40 dataset, manual stereo measurements were subsequently made to the 18 ICPs shown in Figure 3 in order to assess the accuracy of measurements resulting from imagery directly oriented using only information from the GPS/IMU (i.e. no triangulation or ground control).

3.2 Influence of GCPs in triangulation

The second phase of experimentation involved the repeated triangulation of the 20 cm GSD ADS40 dataset using different configurations of GCPs (Figure 4) in order to assess the influence of GCPs in the bundle block adjustment and on resultant measurement accuracy.

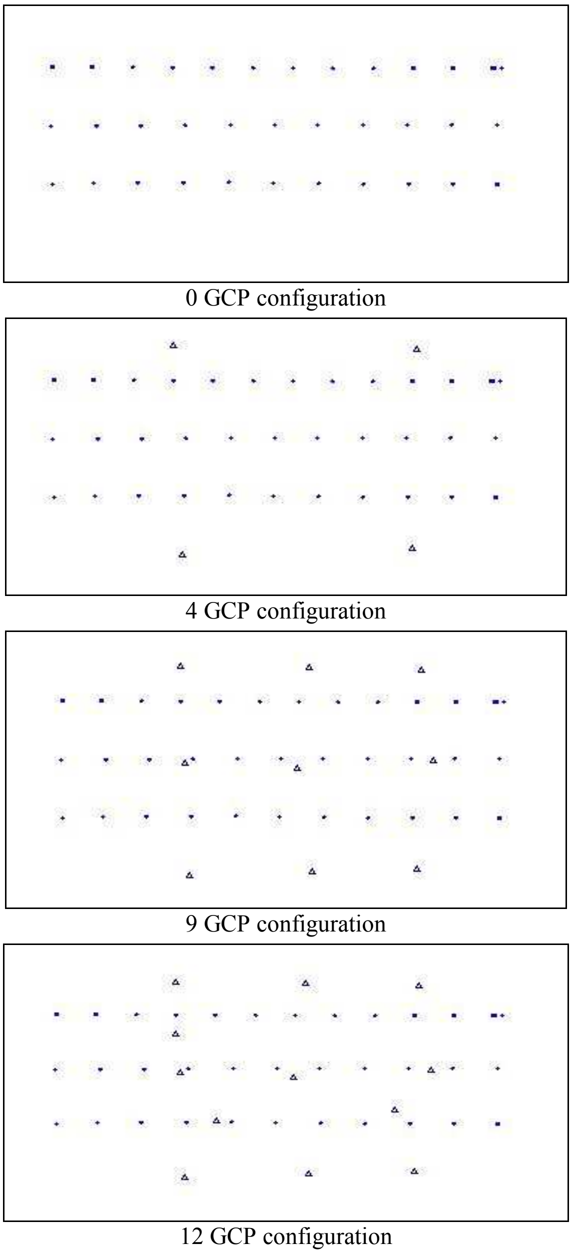

Figure 4. Location of GCPs (triangles) in relation to flight lines represented by IPOS position fixes (blue dots).

The ADS40 imagery of the study area was pre-processed, rectified and triangulated interactively using the ADS40 ground processing software GPro, BAE Systems SOCET SET photogrammetric software suite and Leica Geosystems ORIMA bundle adjustment software (see Tempelmann et al. (2000) and Hinsken et al. (2002) for further generic information on software and triangulation). Forward, nadir and backward panchromatic images were used in each triangulation and the number of GCPs used in triangulation was systematically increased in different configurations, from 0 GCPs through 4, 9 and finally 12 GCPs (Figure 4), resulting in the sigma naught values presented in Table 1.

Configuration	No. of GCPs	σ_0 (μm)
1	0	3.3
2	4	3.4
3	9	3.4
4	12	3.4

Table 1. Indirect sensor orientation precision (σ_0) results for triangulations using different GCP configurations.

Using the forward and backward looking panchromatic images, manual stereo measurements from the triangulated imagery were subsequently made to the same 18 ICPs as measured in the direct orientation assessment described in Section 3.1 (and shown in Figure 3) for each triangulation.

3.3 Influence of flying height on accuracy

The "optimum" procedures for triangulation (9 GCP configuration), as determined from the previous Waldkirch study (Alhamlan et al., 2004), were then applied to the ADS40 panchromatic imagery captured at 15, 25 and 30 cm GSDs. Once orientated (sigma naught values from triangulation are given in Table 2), manual stereo measurement of the 18 ICPs distributed throughout the study area were again used to evaluate the accuracy of planimetric and height coordinates determined for the imagery at different scales. At this stage it should be noted that a different, less experienced, operator performed these experiments to those reported elsewhere in the paper. This is one possible reason for the slightly higher sigma naught values reported in Table 2 as opposed to Table 1.

GSD	No. of GCPs	σ_0 (μm)
15	9	4.5
25	9	3.7
30	9	3.7

Table 2. Indirect sensor orientation precision (σ_0) results for triangulations using different GCP configurations.

3.4 Assessment of photogrammetric products

In order to assess the quality of products resulting from photogrammetric processing, further experimentation examined the automatic extraction of DEMs and creation of orthoimagery from the ADS40 imagery. Only the evaluation of DEM products are reported in this paper.

DEMs of three different terrain types (determined as "flat", "hilly" and "urban") were automatically extracted from the 20 cm GSD ADS40 dataset using forward, nadir and backwards looking images with adaptive and non-adaptive extraction methods and different matching strategies in SOCET SET. Unedited elevation models were compared with DEM data generated by the Optech ALTM 2050 lidar survey.

4. RESULTS

4.1 Accuracy of direct orientation

Table 3 gives the RMS error statistics for measurements made to the 18 ICPs after the ADS40 data has been resampled to remove the influences of the aircraft movement during image acquisition. No triangulation has taken place at this stage, and this solution can be considered to be a direct one that, in theory at least, could be performed in "real-time".

Method	RMS (m)		
	X	Y	Z
Direct orientation	2.039	5.104	0.961

Table 3. X, Y, Z RMS error statistics for Pan FB (42º) manual stereo measurement for directly oriented imagery.

4.2 Influence of GCPs in triangulation

Table 4 shows the results of manual stereo measurement to the 18 ICPs using data from triangulations performed using different numbers of GCPs, as shown in Figure 4.

Config.	No. of GCPs	RMS (m)		
		X	Y	Z
1	0	1.938	5.139	0.915
2	4	0.175	0.357	0.348
3	9	0.188	0.248	0.188
4	12	0.185	0.239	0.194

Table 4. X, Y, Z RMS error statistics for Pan FB (42º) manual stereo measurement for different GCP configurations

4.3 Influence of flying height on accuracy

Table 5 presents the results of triangulations performed using GCP configuration 3 (9 GCPs) for the 15, 25 and 30 cm GSD imagery. Data for the 20 cm imagery has been derived from the tests undertaken in Section 4.2. It has been included in the table, but it should be noted that this imagery was processed and measured by a different operator.

GSD (cm)	RMS (m)		
	X	Y	Z
15	0.135	0.190	0.153
20	0.188	0.248	0.188
25	0.210	0.233	0.268
30	0.228	0.235	0.337

Table 5. X, Y, Z RMS error statistics for Pan FB (42º) manual stereo measurements for imagery of different GSD.

4.4 Assessment of photogrammetric products

Table 6 highlights the results for automatic elevation extraction results compared against the lidar survey.

Although multiple combinations of different extraction methods and matching strategies were employed in SOCET SET, the "non-adaptive" extraction method was found to provide the best results, and it is these that are presented in Table 6. Strategies for this method were "flat dense", "rolling dense" and "steep dense" for "flat", "hilly" and "urban" terrain respectively. Forward, nadir and backward looking panchromatic images were used in each case to generate the DEM. It should be noted that no editing, manual or otherwise, has been performed on either the ADS40 or the ALTM2050 DEMs used.

Terrain	Mean (m)	St. dev. (m)	RMS (m)
"Flat"	-0.535	0.223	0.580
"Hilly"	0.064	0.599	0.602
"Urban"	-1.009	1.322	1.661

Table 6. Error statistics for "flat", hilly and "urban" DEMs extracted from ADS40 data and compared to ALTM 2050 lidar survey.

5. DISCUSSION

5.1 Accuracy of direct orientation

Stereo measurements of ICPs after direct sensor orientation processing produced significant systematic errors in all three axes. Although this trend has been previously noted in other performance studies (e.g. Alhamlan et al., 2004, Cramer, 2005), particularly for the Z axis, the magnitude of the errors seen here are significantly larger than previously observed. This is particularly evident in the results for the planimetric coordinates and is almost certainly due to the peculiarities of the OSGB36 coordinate system used to perform the check measurements. The WGS84 system used in the direct orientation is a modern global coordinate system and the OSGB36 national grid system is a 1936 system traditionally used for mapping in Britain. The later has significant distortions distributed across the country, thus indirect orientation and the importing of GCPs is necessary as the required solution to solve this problem.

5.2 Influence of GCPs in triangulation

The results from Table 4 are presented again in Figure 5 for emphasis.

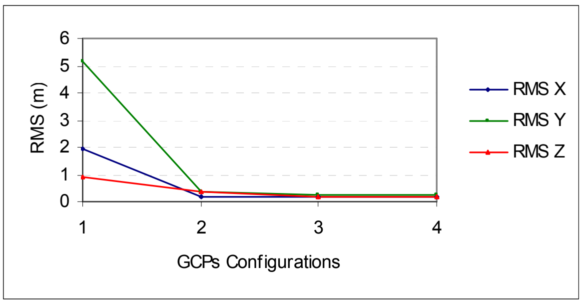

Figure 5. X, Y, Z RMS error statistics for Pan FB (42º) manual stereo measurement for different GCP configurations

Results here were broadly consistent with the findings of Alhamlan et al. (2004), which was carried out using another ADS40 sensor system for a different study area (Waldkirch in Switzerland). These two empirical case studies have both shown that, despite advances made in direct positioning and orientation using integrated satellite and inertial surveying, the importing of GCPs into the block adjustment process remains a critical issue influencing the achievable planimetric and height accuracy during subsequent photogrammetric measurement. Indeed little improvement is seen in the triangulated 0 GCP configuration over the directly oriented imagery.

As soon as GCPs are introduced into the triangulation, the RMS in both plan and height decreases significantly. The use of four GCPs, one in each corner of the block, has previously been shown (Alhamlan et al., 2004) to adequately "nail down" the block, minimising errors resulting from the datum shift between the GPS/IMU and the ground control system. In this case some improvement is evident in the triangulations that adopted a higher number of GCPs. This can again be attributed to the peculiarities of the OSGB36 ground coordinate system used.

The theoretical planimetric and height precisions for measurements made using imagery derived from the sensor in this configuration (assuming the nominal 0.20 m GSD, 26˚ forward / 16˚ backward look angle) are 0.10 m and 0.13 m respectively (note, these nominal values are scaled by the sigma naught value derived from triangulation of 3.4 µm). This is based on the classical theory for analogue cameras and is not necessarily suited to the three-line sensor used here; however it provides a useful benchmark against which the sensor can be assessed.

Whilst the sensor data does not quite reach the theoretical computed level of performance, a number of factors can be considered as contributing to this. For example, the targets used as ICPs were natural detail points coordinated by standard GPS survey procedures (which in itself will contain errors). Moreover, the imagery was processed and measured by inexperienced photogrammetric operators in the form of research students. In cases where significantly more, better coordinated, signalised ICPs exist, e.g. the independent Vaihingen/Enz test presented by Cramer (2005), empirical results can be expected to be significantly better than the values presented herein. Nevertheless, these results might be considered to be typical of day-to-day mapping use of the sensor. The sensors ability to produce homogeneous accuracy in X, Y and Z axes (essentially due to the long base created by the 42˚ stereo angle) is impressive, the Z RMS indicating an error better than 0.01% of the flying height. This figure is directly comparable to established values expected when using film imagery from conventional mapping cameras (Read and Graham, 2002).

5.3 Influence of flying height on accuracy

Sigma naught values for the 15, 25 and 30 cm datasets were higher than the 20 cm dataset. In general this may be attributed to a different, less experienced, operator performing the observations. The relatively high sigma naught value for the 15 cm dataset could be due to the fact that there are four strips covering the study area, rather than three in the case of the 20 cm dataset and two for both the 25 and 30 cm datasets. Alternatively, the fact that, at 15 cm, the sensor is performing beyond its original designed "optimum" GSD of 20 cm may be influencing the results.

The data from Table 5 is presented again in Figure 6. It can be seen that the general rule held that there is a direct linear relationship between the resulting measurement accuracy and the ground resolution of the input imagery. Figures should be compared with the theoretical precisions of 0.10 m, 0.10 m, 0.14 m and 0.17 m for planimetry and 0.13 m, 0.13 m, 0.18 m and 0.22 m for height from 15, 20, 25 and 30 cm GSDs respectively (calculated as described in Section 5.2 using scaling from appropriate sigma naught values derived through triangulation).

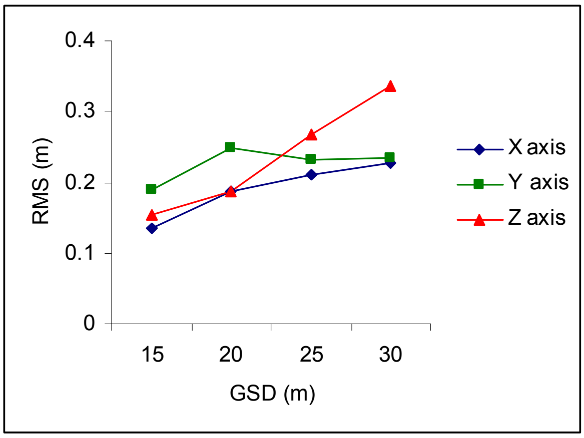

Figure 6. X, Y, Z RMS error statistics for Pan FB (42º) manual stereo measurement for different GSDs.

Again, the sensor does not quite perform at this theoretical level, showing height errors at approximately 0.01 % of the flying height at the "optimal" 20 cm GSD, and falling off slightly either side of this. Although, from the calculated theoretical figures, the 15 cm GSD dataset should not necessarily produce data of better quality than the 20 cm GSD data (due to the worse sigma naught value provided from triangulation), it does, as might logically be expected, generate data of improved quality in all three coordinate axes (albeit slightly degraded when regarded as a percentage of flying height).

5.4 Assessment of photogrammetric products

Despite non-synchronous data capture and the fact that no editing had been performed on any of the elevation models, good consistency was observed between the ALTM 2050 lidar and ADS 40 DEMs in both "flat" and "hilly" terrain, with RMS height errors between the two surveys of approximately 0.6 m (three pixels). Urban terrain, as expected, proved more problematic, with the best RMS error achieved being only 1.6 m (eight pixels).

6. CONCLUDING REMARKS

Airborne sensors of the type investigated are still in their infancy, and future work is necessary in order to overcome problems and issues which remain and ensure that advances in processing software are incorporated into the workflow. Nevertheless, this independent research has permitted a series of initial conclusions to be drawn about the performance of the sensor in a "real-world" mapping environment. Based on the findings of this research, preliminary recommendations can be made for the optimum deployment of the ADS40 sensor under similar operational conditions. The results should be of interest to both researchers and practitioners currently engaged in the assessment of airborne digital sensors.

ACKNOWLEDGEMENTS

The results presented in this paper summarise the findings from postgraduate research programmes undertaken at the University of Newcastle upon Tyne by Saad Alhamlan and Ahmed Abuoliat. On behalf of these former research students and the University of Newcastle upon Tyne, the corresponding author would like to acknowledge the support (data, software and expertise) that was provided throughout these programmes by both Leica Geosystems and Ordnance Survey.

REFERENCES

Alhamlan, S., Mills, J. P., Walker, A. S. and Saks, T., 2004. The influence of ground control points in the triangulation of Leica ADS40 data. *The International Archives of the Photogrammetry, Remote Sensing and Spatial Information Sciences,* XXXV, Part B1, pp. 495–500.

Cramer, M., 2005. 10 years ifp test site Vaihingen/Enz: an independent performance study. In: Fritsch, D. (Ed.), Photogrammetric Week '05. Wichmann, Karlsruhe, pp. 79-92.

Hinsken, L., Miller, S., Templemann, U., Uebbing, R. and Walker, S., 2002. Triangulation of LH-Systems' ADS40 imagery using ORIMA GPS/IMU. *The International Archives of the Photogrammetry, Remote Sensing and Spatial Information Sciences*, Graz, Austria, Vol. XXXIV, Part 3A, pp. 156-162.

Read, R. And Graham, R., 2002. *Manual of aerial survey: primary data acquisition.* Whittles Publishing, Caithness, Scotland, pp. 165.

Sandau, R., Braunecker, B., Driescher, H., Eckardt, A., Hilbert, S., Hutton, J., Kirchhofer, W., Lithopoulos, E., Reulke, R. and Wicki, S., 2000. Design Principles of the LH Systems ADS40 Airborne Digital Sensor. *The International Archives of the Photogrammetry, Remote Sensing and Spatial Information Sciences*, Amsterdam, The Netherlands, Vol. XXXIII, Part B2, pp. 258-265.

Tempelmann, U., Börner, A., Chaplin, B., Hinsken, L., Mykhalevych, B., Miller, S., Recke, U., Reulke, R. and Uebbing, R., 2000. Photogrammetric software for the LH Systems ADS40 Airborne Digital Sensor. *The International Archives of the Photogrammetry, Remote Sensing and Spatial Information Sciences*, Amsterdam, The Netherlands, Vol. XXXIII, Part B2, pp. 552-559.